



ELSEVIER

Contents lists available at ScienceDirect

Ceramics International

journal homepage: www.elsevier.com/locate/ceramint

Synthesis, structure and luminescent properties of Eu^{3+} doped $\text{Ca}_3\text{LiMgV}_3\text{O}_{12}$ color-tunable phosphor

Xinguo Zhang^{a,b,*}, Zhenpeng Zhu^a, Ziying Guo^a, Zishan Sun^a, Liya Zhou^b, Zhan-chao Wu^c

^a Guangdong Provincial Key Laboratory of New Drug Screening, School of Pharmaceutical Sciences, Southern Medical University, Guangzhou 510515, China

^b School of Chemistry and Chemical Engineering, Guangxi University, Nanning 530004, China

^c State Key Laboratory Base of Eco-chemical Engineering, Laboratory of Inorganic Synthesis and Applied Chemistry, College of Chemistry and Molecular Engineering, Qingdao University of Science and Technology, Qingdao 266042, China

ARTICLE INFO

Keywords:

Vanadate
 $\text{Ca}_3\text{LiMgV}_3\text{O}_{12}$
 Structure
 Color-tunable

ABSTRACT

A new vanadate $\text{Ca}_3\text{LiMgV}_3\text{O}_{12}$ and its Eu^{3+} -doped counterparts were synthesized. Rietveld refinement result of $\text{Ca}_3\text{LiMgV}_3\text{O}_{12}$ host indicates that it belongs to cubic space group Ia-3d with parameters of $a = 12.4300 \text{ \AA}$, $V = 1920.49 \text{ \AA}^3$, $Z = 8$. Under UV excitation, pure $\text{Ca}_3\text{LiMgV}_3\text{O}_{12}$ exhibits a bluish-green broadband emission at 490 nm, while Eu^{3+} doped $\text{Ca}_3\text{LiMgV}_3\text{O}_{12}$ shows one bluish-green broad band with a series of red sharp peaks, which originate from the $\text{V}^{5+} \cdot \text{O}^{2-}$ charge transfer and the Eu^{3+} intra-4f transitions, respectively. The occurrence of $\text{VO}_4 \rightarrow \text{Eu}^{3+}$ energy transfer is confirmed by decay lifetime analysis and time-resolved emission spectra. It is found that emitting color varies from bluish-green to orange-red with increasing Eu^{3+} concentration. VO_4 bluish-green and Eu^{3+} red emission shows different thermal quenching response with increasing temperature, due to their different activation energy.

1. Introduction

Vanadates are a kind of well-known self-activated luminescent materials, which have intense UV absorption band and efficient visible emission band, due to $\text{V}^{5+} \cdot \text{O}^{2-}$ charge transfer transition [1–3]. Novel vanadate phosphors with good luminescent properties, i.e. $\text{Cs}_5\text{V}_3\text{O}_{10}$, $\text{Ca}_5(\text{Mg}/\text{Zn})_4(\text{VO}_4)_6$, and $(\text{K}/\text{Rb}/\text{Cs})\text{VO}_3$, have been reported in recent years [4–6]. A series of garnet-structured vanadates with composition of $\{\text{Ca}_2\text{Na}/\text{K}\}[\text{M}]_2\text{V}_3\text{O}_{12}$ were reported by Bayer et al., where $\text{Ca}^{2+}/\text{Na}^+/\text{K}^+$ is located in a 8-fold dodecahedral site, M^{2+} ($\text{M} = \text{Mg}^{2+}/\text{Co}^{2+}/\text{Ni}^{2+}/\text{Cu}^{2+}/\text{Zn}^{2+}$) is 6-coordinated and V^{5+} is 4-coordinated with O^{2-} anions [7]. The vanadate garnet ($\text{Ca}_2\text{Na}/\text{KMg}_2\text{V}_3\text{O}_{12}$) exhibits a strong broadband emission under UV excitation, due to the ${}^3T_1-{}^1A_1$ ($J = 1, 2$) transitions of VO_4 group [8].

Cationic/anionic substitutions have been extensively used for exploring new and highly efficient solid-state luminescent materials. By substituting $\text{Na}/\text{K}[\text{M}]_2$ in $\{\text{Ca}_2\text{Na}/\text{K}\}[\text{M}]_2\text{V}_3\text{O}_{12}$ by CaLiM ($\text{M} = \text{Mg}$), a new vanadate with composition of $\text{Ca}_3\text{LiMgV}_3\text{O}_{12}$ is prepared. By introducing rare-earth (RE) ions into vanadate host, the phonon-assisted energy transfer from VO_4 to RE ions can occur and both VO_4 and RE emissions can be simultaneously observed. As far as we know, the electronic and crystal structure, as well as luminescent properties of $\text{Ca}_3\text{LiMgV}_3\text{O}_{12}$ and its Eu^{3+} -doped counterparts have not been

systemically studied. In this work, crystal structure of $\text{Ca}_3\text{LiMgV}_3\text{O}_{12}$ is investigated by XRD Rietveld refinement, and the corresponding electronic structure is obtained by DTF stimulation. Due to $\text{VO}_4 \rightarrow \text{Eu}^{3+}$ energy transfer, $\text{Ca}_3\text{LiMgV}_3\text{O}_{12}:\text{Eu}^{3+}$ exhibits both VO_4 blue emission and Eu^{3+} red emission, whose emitting color could be tuned by Eu^{3+} concentration. The corresponding energy transfer process was also discussed through decay lifetime analysis and time-resolved emission spectra.

2. Experimental

2.1. Synthesis

All samples were synthesized by high-temperature solid-state method. Stoichiometric amounts of raw compounds, i.e. CaCO_3 , Li_2CO_3 , $\text{Mg}(\text{OH})_2 \cdot 4\text{MgCO}_3 \cdot 5\text{H}_2\text{O}$, NH_4VO_3 and Eu_2O_3 , were mixed according to $(\text{Ca}_{1-x})_3\text{LiMgV}_3\text{O}_{12} \cdot 3x\text{Eu}^{3+}$ ($x = 0, 0.01, 0.03, 0.05, 0.07, 0.09$ and 0.11 , respectively), and grounded for 15 min. The mixtures have been pre-heated at $600 \text{ }^\circ\text{C}$ for 2 h, cooled to room temperature, then re-grounded into powder and calcinated at $900 \text{ }^\circ\text{C}$ in air atmosphere for 6 h.

* Corresponding author at: Guangdong Provincial Key Laboratory of New Drug Screening, School of Pharmaceutical Sciences, Southern Medical University, Guangzhou 510515, China. E-mail addresses: panzer@smu.edu.cn, mppc1@qq.com (X. Zhang).

<https://doi.org/10.1016/j.ceramint.2018.06.069>

Received 1 June 2018; Received in revised form 8 June 2018; Accepted 9 June 2018
 0272-8842/ © 2018 Elsevier Ltd and Techna Group S.r.l. All rights reserved.

2.2. Characterizations

X-ray diffraction (XRD) patterns of all phosphors were examined by D8 (Bruker) X-ray diffractometer. The composition and structure of pure $\text{Ca}_3\text{LiMgV}_3\text{O}_{12}$ sample is determined from XRD refinement using TOPAS Rietveld refinement software. UV–vis diffuse reflectance spectra (DRS) were collected using UV-3600 (Shimadzu) UV–Vis spectrometer. The photoluminescence (PL) and PL excitation (PLE) spectra, luminescence decay lifetimes, time-resolved emission spectra (TRES), temperature-dependent PL spectra and quantum yield (QY) were measured by FLS920 (EDINBURGH) spectrometer. Electronic structure of $\text{Ca}_3\text{LiMgV}_3\text{O}_{12}$ was studied by DFT calculation using VASP software. Calculation set-up and details are similar with that Ref. [9].

3. Results and discussion

3.1. Crystal Structure for $\text{Ca}_3\text{LiMgV}_3\text{O}_{12}$

Since the crystal structure of $\text{Ca}_3\text{LiMgV}_3\text{O}_{12}$ has not been reported in previous papers, the iso-structural $\text{Ca}_2\text{NaMg}_2\text{V}_3\text{O}_{12}$ (Ia-3d space group, $a = 12.427 \text{ \AA}$, $V = 1919.1 \text{ \AA}^3$, $Z = 8$) was chosen to be the initial model in Rietveld analysis. After some trial and error, it is found that the Rietveld profile fits experimental XRD pattern best when Na is substituted by Ca and one of Mg is replaced by Li in $\text{Ca}_2\text{NaMg}_2\text{V}_3\text{O}_{12}$. Fig. 1 shows XRD profile of $\text{Ca}_3\text{LiMgV}_3\text{O}_{12}$ for Rietveld refinement. The final crystallographic and refinement parameters of $\text{Ca}_3\text{LiMgV}_3\text{O}_{12}$ are listed in Table 1. The refinement results indicate that the $\text{Ca}_3\text{LiMgV}_3\text{O}_{12}$ is of cubic structure with cell parameters of $a = 12.4300 \text{ \AA}$, $V = 1920.49 \text{ \AA}^3$, $Z = 8$, which is slightly larger than $\text{Ca}_2\text{NaMg}_2\text{V}_3\text{O}_{12}$.

Fig. 2 shows the structure diagram of $\text{Ca}_3\text{LiMgV}_3\text{O}_{12}$ according to the refinement data. Every V-O tetrahedron is constituted by one V and four O, while the Ca and Mg is 8- and 6-coordinated. Due to similar ionic radius between Li^+ ($r_{\text{Li}} = 0.76 \text{ \AA}$) and Mg^{2+} ($r_{\text{Mg}} = 0.72 \text{ \AA}$), it is reasonable that Li^+ ions occupy Mg site and form $[\text{LiO}_6]$ octahedron, while the Na^+ and K^+ ions occupy Ca^{2+} site and form $[\text{Na/KO}_6]$ dodecahedron. The difference in alkali ions occupied site might have great effect on the corresponding luminescent properties.

3.2. Electronic structure of $\text{Ca}_3\text{LiMgV}_3\text{O}_{12}$

Fig. 3a shows the calculated band structure of $\text{Ca}_3\text{LiMgV}_3\text{O}_{12}$. It is found that the valence bands maximum and the conduction bands minimum are located at the same G point, and $\text{Ca}_3\text{LiMgV}_3\text{O}_{12}$ exhibits a direct band gap (E_g) of about 3.70 eV. With wide band gap (3.0–6.0 eV), $\text{Ca}_3\text{LiMgV}_3\text{O}_{12}$ could be appropriate for doping activator ions, since

both the excited and ground state of dopant will be located between conduction and valence band.

To further probe the energy bands composition, the total- and partial-density of states (TDOS/PDOS) of $\text{Ca}_3\text{LiMgV}_3\text{O}_{12}$ were calculated. As seen in Fig. 3b, the valence bands maximum is mainly formed by O-2p state with a tiny contribution of Mg-2p state. Meanwhile, the conduction bands minimum is dominated by V-3d state in addition to Ca-3p and Mg-2p states. Thus, the host absorption of $\text{Ca}_3\text{LiMgV}_3\text{O}_{12}$ is assigned to the charge transitions between O-2p and V-3d state.

Diffuse reflectance spectra of pure $\text{Ca}_3\text{LiMgV}_3\text{O}_{12}$ and Eu^{3+} doped $\text{Ca}_3\text{LiMgV}_3\text{O}_{12}$ are shown in Fig. 4. An obvious drop at $\sim 300 \text{ nm}$ is observed in the DRS of pure $\text{Ca}_3\text{LiMgV}_3\text{O}_{12}$, which could be attributed to the band transition of $\text{Ca}_3\text{LiMgV}_3\text{O}_{12}$ host. Along with 300 nm absorption band, Eu^{3+} doped $\text{Ca}_3\text{LiMgV}_3\text{O}_{12}$ also exhibit some weak absorption peaks at 395, 464 and 535 nm, which could be attributed to $\text{Eu}^{3+} {}^7F_0 \rightarrow {}^5L_6/{}^5D_2/{}^5D_1$ transitions.

The experimental band gap (E_g) value is estimated through DRS as followed:

$$(ah\nu)^n = A(h\nu - E_g) \quad (1)$$

Where $h\nu$, a and A stands for incident photon energy, absorption coefficient and the constant, respectively. The n value is chosen as 2 in case of direct transition. The absorption coefficient a is obtained by using the observed reflectance (R) in the DRS:

$$a = \frac{(1 - R)^2}{2R} \quad (2)$$

Thus, $(ah\nu)^2$ values are plotted with the photon energy axis in Fig. 4 inset. The E_g value ($\sim 3.50 \text{ eV}$) is found as the crossing point of liner fitting and the photon energy axis, which is close to theoretical calculated value (3.70 eV).

3.3. Luminescent properties of $\text{Ca}_3\text{LiMgV}_3\text{O}_{12}$

Fig. 5a presents PL and PLE spectra of pure $\text{Ca}_3\text{LiMgV}_3\text{O}_{12}$. PLE spectrum consists of a main broadband at 330 nm along with shoulder at 280 nm, which is due to charge transitions in VO_4^{3-} tetrahedron. Two fitting peaks at 300 and 340 nm could be assigned to ${}^1A_1 \rightarrow {}^1T_j$ transitions ($j = 2$ and 1), respectively. PL spectrum of pure $\text{Ca}_3\text{LiMgV}_3\text{O}_{12}$ demonstrates a broad emission band with peak at 490 nm and full width at half maximum of 141 nm, which could be further decomposed into two sub-peaks at 481 and 554 nm due to ${}^3T_j \rightarrow {}^1A_1$ transitions ($j = 2$ and 1), respectively. By comparison, the maximum emitting peak is about 520 and 528 nm for $\text{Ca}_2\text{NaMg}_2\text{V}_3\text{O}_{12}$ [10] and $\text{Ca}_2\text{KMg}_2\text{V}_3\text{O}_{12}$ [11]. The reason of different emission maximum wavelength could be attributed to the different alkali ions occupied site in the vanadate structure: when Li^+ ions occupy 6-coordinated Mg site, the non-radiative relaxation of excited electron in VO_4^{3-} tetrahedron could be restrained, and more excited electrons at higher levels will return to ground state through radiative transition, which results in emission blue-shift of $\text{Ca}_3\text{LiMgV}_3\text{O}_{12}$.

Decay curves of pure $\text{Ca}_3\text{LiMgV}_3\text{O}_{12}$ sample at 330 nm excitation are depicted in Fig. 5b, which could be fitted with bi-exponential equation:

$$I(t) = I_0 + A_1 \exp(-t/\tau_1) + A_2 \exp(-t/\tau_2) \quad (3)$$

I_0 and $I(t)$ stands for initial emission intensity and emission intensity at time t ; τ_1 and τ_2 stands for fast and slow lifetime components; A_1 and A_2 stands for different constants. Thus, the effective decay time τ^* could be obtained by:

$$\tau^* = \frac{A_1 \tau_1^2 + A_2 \tau_2^2}{A_1 \tau_1 + A_2 \tau_2} \quad (4)$$

Therefore, effective decay time of $\text{Ca}_3\text{LiMgV}_3\text{O}_{12}$ emission was calculated to be 17.37 μs .

The temperature-dependent PL spectra of $\text{Ca}_3\text{LiMgV}_3\text{O}_{12}$ phosphor

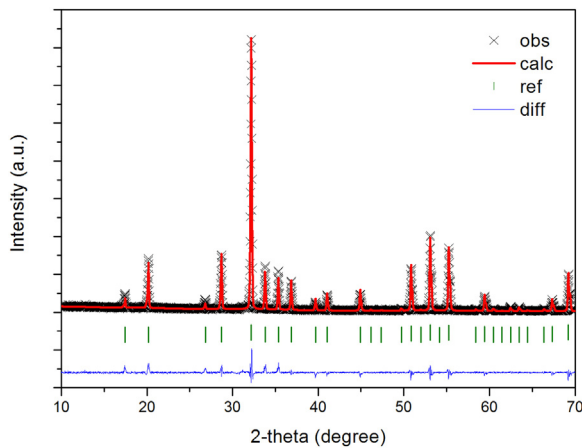


Fig. 1. Rietveld refinement of the powder X-ray diffraction profile of $\text{Ca}_3\text{LiMgV}_3\text{O}_{12}$. Data (cross) and fit (line), the difference profile, and expected reflection positions are displayed.

Download English Version:

<https://daneshyari.com/en/article/7885963>

Download Persian Version:

<https://daneshyari.com/article/7885963>

[Daneshyari.com](https://daneshyari.com)